A STUDY OF HYDROGEN FLAME LENGTH WITH COMPLEX NOZZLE GEOMETRY

Henriksen, M.[1], Gaathaug, A.V.[1] and Lundberg, J.[1]
[1] Faculty of Technology, Natural Sciences and Maritime Sciences, University College of Southeast Norway, Kjølnes Ring 56, Porsgrunn, 3901, Norway

ABSTRACT

The growing number of hydrogen fillings stations and cars increases the need for accurate models to determine risk. The effect on hydrogen flame length was measured by varying the diameter of the spouting nozzle downstream from the chocked nozzle upstream. The results was compared with an existing model for flame length estimations. The experimental rig was setup with sensors that measured accurately temperature, mass flow, heat radiation and the pressure range from 0.1 to 11 MPa. The flame length was determined with an in-house developed image-processing tool, which analyzed a high-speed film of the each experiment. Results show that the nozzle geometry can cause a deviation as high as 50% compared to estimated flame lengths by the model if wrong assumptions are made. Discharge coefficients for different nozzles has been calculated and presented.

1.0 INTRODUCTION

In 2015, 54 new hydrogen refuelling stations was built worldwide creating a total 214 fully operate refuelling stations with even more planning to be built [1]. This increases the demand of reliable physical models, engineering models and risk analysis. Projects such as the Susana Project is a great example that shows the importance of validated models when estimating potential risk [2]. There is a possibility of a hydrogen leakages from flanges, holes and broken pipes etc. and the possibility of ignition is high, due to the low minimum ignition energy of hydrogen. The length of these hydrogen jet flames will have an impact on the risk and safety analysis.

Previous experiments with hydrogen flames lengths show a relationship between pressure and nozzle diameter [3, 4]. These experiments have then related the flame length only to be dependent on mass flow, since mass flow is a function of nozzle diameter and pressure. For safety valves, the spouting nozzle (downstream nozzle) can have a higher nozzle diameter then the mass determining nozzle (upstream/chocked nozzle). This was found during an investigation of an accidental release of hydrogen due to a failure of a gas regulator with a safety valve [5]. The influence of the "complex" geometry on the hydrogen flame length is the focus of this study.

Several models for estimating flame lengths of hydrogen are developed for both buoyant and under expanded jets. [3, 4, 6, 7, 8] These models are based upon expansion of hydrogen through one orifice and the flame length with respect to the either pressure and nozzle diameter or mass flow and nozzle diameter. In this study, the HySafer model (equation 1) by Saffers and Molkov was chosen for comparison. The difference between the HySafer model and other models is that it is based upon a large collection of data from several different experiments and the model also includes nozzle diameter.

$$L_f = 54\left(\dot{m}\cdot dz\right)^{0.312} \tag{1}$$

where L_f – flame length, m, $\dot{m}$; – mass flow, kg/s; dz – nozzle diameter, m.

The results from each experiment was obtain by recording the hydrogen flame (with a known nozzle configuration) with a high-speed camera, pressure, mass-flow and temperature sensors. An in-house developed image-processing tool in Matlab was then use to determine the flame length.

2.0 EXPERIMENTAL METHOD

Fig 1 show the experimental setup where the hydrogen was supplied from a 20 MPa cylinder. A pressure regulator with a range from 1.0 to 12 MPa controlled the pressure. The maximum pressure was set to 10MPa due to the pressure rating on the Coriolis mass flow meters and the flexible hose from the regulator. A Coriolis mass flow meter from Micro-Motion was used to accurately measure the mass flow of hydrogen. A pressure sensor close to the nozzle is mounted to get the pressure before the nozzle. The nozzle unit with interchangeable nozzles was mounted on an aluminium table. A row of radiation sensors was mounted for future use.

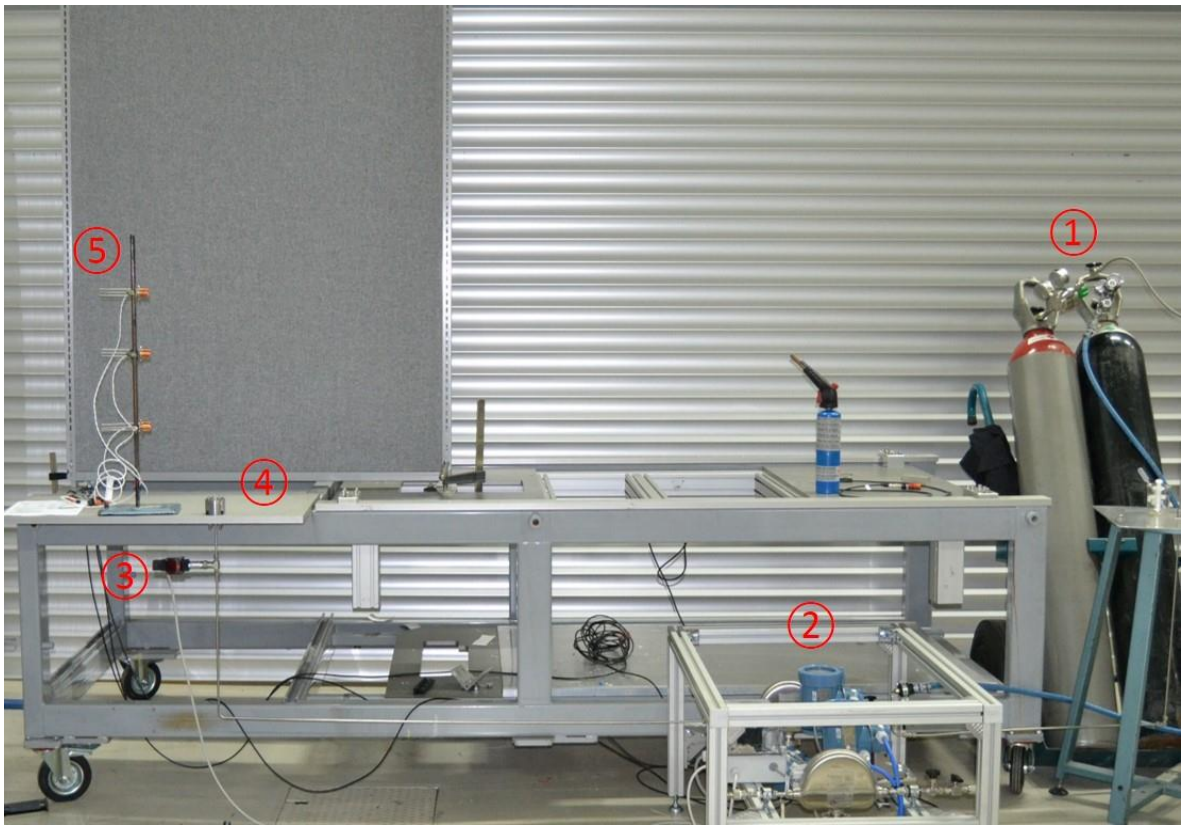

Figure 1. The experimental setup: 1) Hydrogen gas cylinder, 2) mass flow meter, 3) pressure sensor, 4) nozzle unit with changeable nozzle configurations, 5) radiation sensors (currently not in use).

The flame was captured using a colour high-speed camera with frame rate of 250 per second (fps). The data from the logging instruments, such as mass flow meter, pressure sensors etc, was synchronized with the camera and recorded at 2000 Hz. Each experiment had a duration of 5 seconds after the system had stabilized, which took approximately 2-4 seconds after ignition. For each experiment, 1250 images and 9999 data points for each sensors was stored. Afterwards the image was analysed with an in-house image-processing tool to determine the flame length. The flame length was determined to be from the nozzle exit (top of the downstream nozzle) to the tip of the flame.

When each data point and all images of a movie is processed for an experiment, an average value for each data series (pressure, mass flow, etc.) and image is produced together with a distribution plot of all flame lengths. The average value for each experiment is then compared with the HySafer model. The relative deviation was calculated with equation 2.

$$REL\_DEV = \left| \frac{(X_{data} - X_{calc})}{X_{data}} \right| \bullet 100\% \qquad (2)$$

where *REL_DEV* – Relative deviation, %, X_{data} – measured value, [-], X_{calc} – calculated value, [-].

2.1 Nozzle configuration

Fig. 2 show the mechanical drawing of the complete nozzle configuration and arrangement. The upstream and downstream nozzle is interchangeable and have a specific bore diameter, which determines the orifice/nozzle size. In this experiment, nozzle diameters of 0.0005m, 0.0010m, 0.0020m and 0.0040m was tested. As Fig. 2 show, the interchangeable nozzles can be stacked on top of each other and hold together by the nozzle housing and bolts. High-pressure seals/packings insured that there was minimal to no leakage during each experiment. The seals/packings were change when new nozzle arrangement was tested.

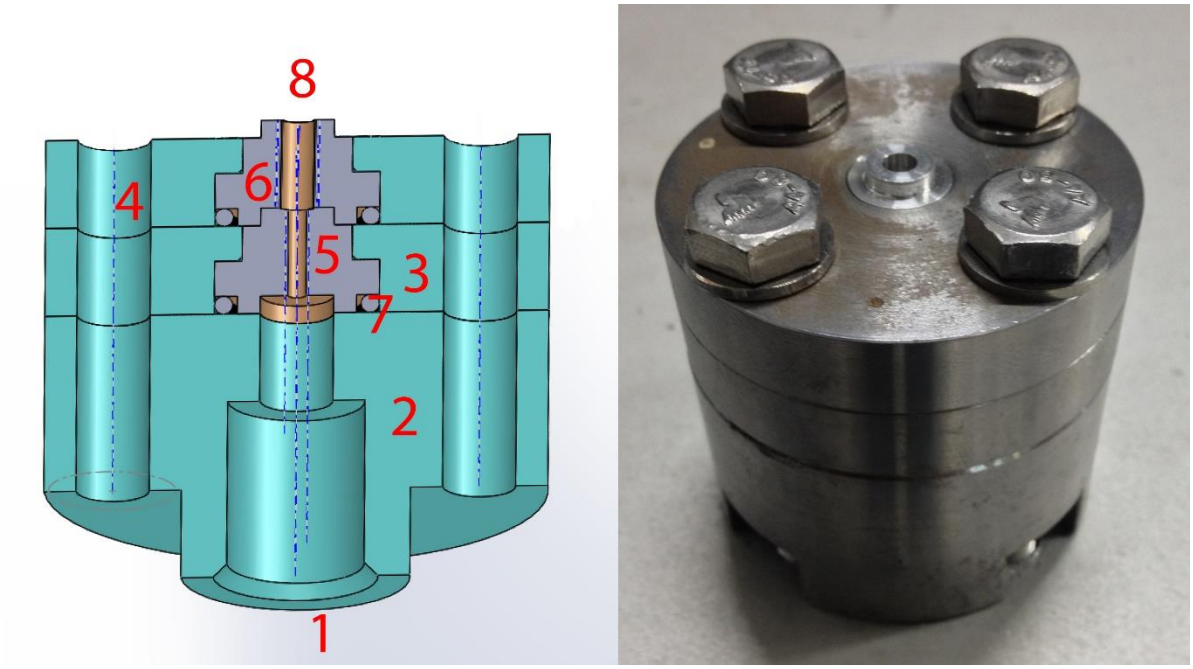

Figure 2. Left: Mechanical drawing of nozzle configuration: 1) Gas inlet and pipe connection, 2) Base housing, 3) Nozzle housing, 4) Bolt threading, 5) Upstream nozzle 6) Downstream nozzle 7) Seal/Packing, 8) Gas outlet, right: Experimental nozzle setup.

2.1 Image-processing tool

To transfer each image from the movie of the hydrogen flame to a numerical value, an image-processing tool was developed in Matlab. The tool have the possibility to find the flame length in every image of the movie, not just the average height from the experiment. From this, one can illustrate the variation of flame length with respect to time, show the distribution of flame lengths over the period analyzed as well as minimum and maximum flame length during the experiment.

The procedure of the image-processing tool explained in steps. The threshold procedure is explained in more detailed after the steps below.

1. Read RAWW image from movie.
2. Convert image to numerical values for each color (RGB)
3. Threshold image
4. Create binary image based on threshold
5. Find flame length in binary image
6. Store flame length
7. Write 16bit image with flame length

Thresholding the image is the most crucial part of the image processing. The threshold value is the set point which distinguishes background noise from signal. Background noise in the image can be mistaken for a flame if the procedure for thresholding is to crude. Thru several tests with manual/visual verification, the procedure for thresholding showed good correlation between manually finding the flame length in the images.

This work used an iterative method to find the threshold value in each image of the movies. The initial threshold was set by averaging a small area in the bottom right corner of the image where only the background was present and adding this with two times its standard deviation.

A new threshold was found by averaging the area around the largest object found (the flame) with initial threshold and adding it with three times its standard deviation. The factor of three was used since it gave better results than with lower multipliers. The change in threshold was then checked. If the deviance was lower than the set error limit, threshold was found, if not, the new threshold was substituted for initial threshold and the procedure was repeated until the change in threshold was lower than the set error limit.

To reduce the computation time only the red image was analyzed for the whole data set, but it was thoroughly investigated that each color gave close to identical flame lengths. The red color was chosen above the other colors since it had a higher intensity. Fig. 3 below show the average flame length of three experiments with all three colors used to determine the flame length. The horizontal lines in the Fig 3 indicates the identified flame length with the line color corresponding to the color analyzed.

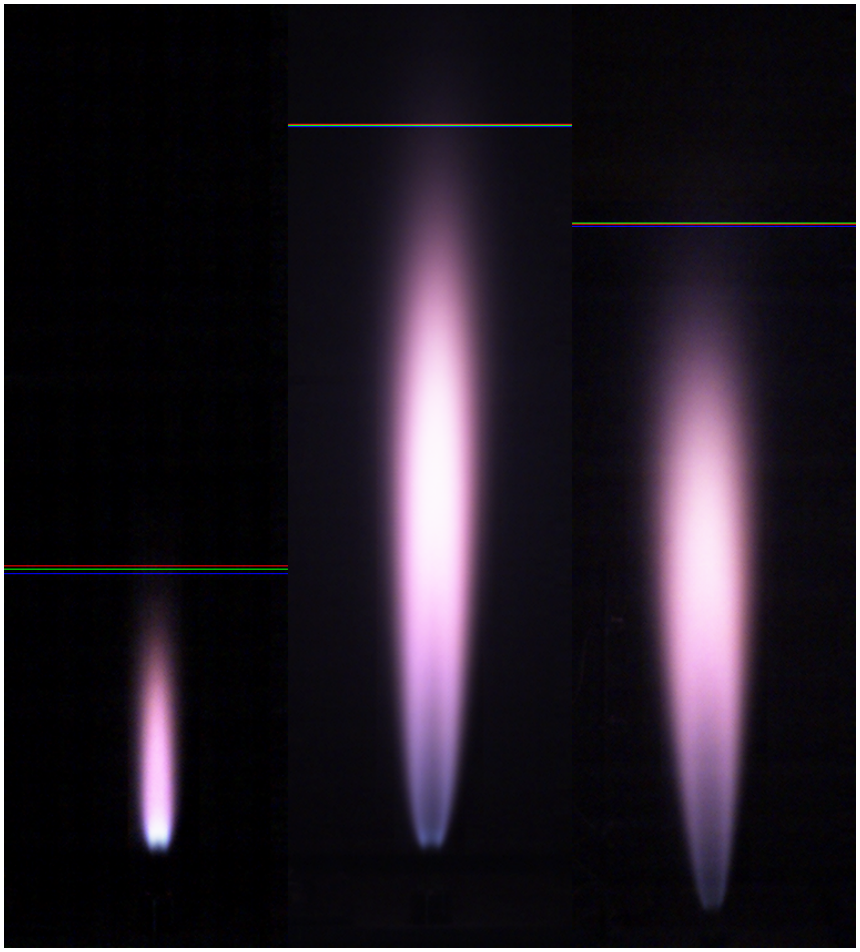

Figure 3. Average flame length for three experiments with red, green and blue colour analysed. Left: 0.0005m nozzle, middle: 0.0010m nozzle, right: 0.0020m nozzle

Table 1 below show the average flame length measured from the whole movie, for each color, for the three images shown in Fig. 3.

Table 1. Comparison of average flame length between different colors in images.

Nozzle diameter [m]	Red image flame length [m]	Green image flame length [m]	Blue image flame length [m]	Largest difference in flame length [m]
0.0005	0.4042	0.3993	0.3949	0.0093
0.0010	1.0627	1.0621	1.0599	0.0028
0.0020	1.3792	1.3815	1.3749	0.0066

As seen in Table 1, the difference in flame length between the three colors in the images is from 0.0028m to 0.0093m. The relative deviation between the largest differences in flame length and the average flame length of the three colors in the image (0.3995m) is for the shortest flame only 2.33%.

For each movie/experiment analyzed, every 25 image was stored with a red line indicating the flame length for visual/manual verification that the tool was working properly. Fig. 4 show on the left a random image from a movie with the red lines showing the identified flame length and lift off, and on the right a plot of the flame length distribution of the same experiment.

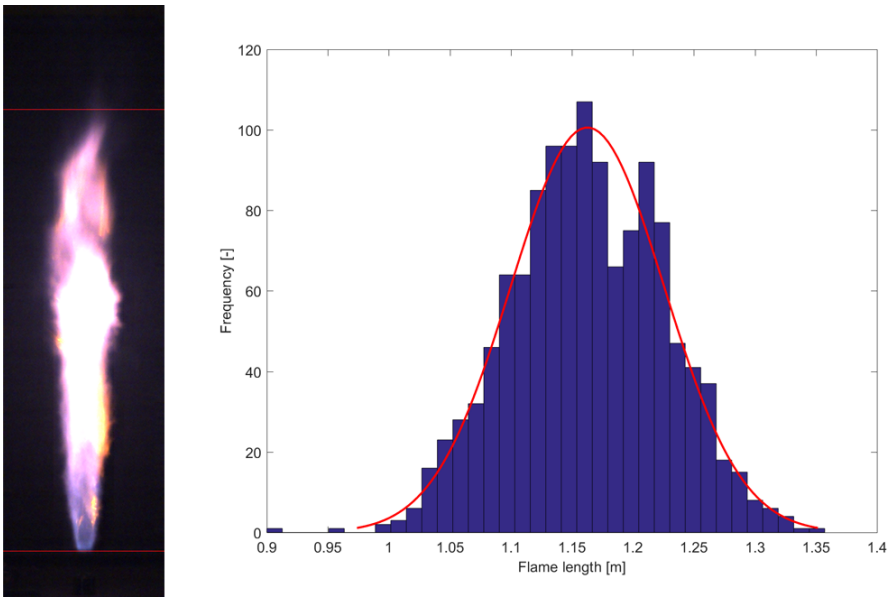

Figure 4. Left – random image from movie/experiment with flame length and lift off indicated, right – histogram plot of a complete experiment

The right image in Fig. 4 show that the flame length of an experiment is normally distributed. The distribution for all experiments showed the same distribution, with only small deviation, indicating that the flame length of hydrogen jet is normally distributed. This means that the standard deviation of the flame length can be used to calculate the most likely minimum and maximum flame length that could be expected.

3.0 RESULT

To verify that nozzle geometry actually has an influence on flame length each nozzle diameter was characterize as a reference. The single nozzle configuration was compared with HySafer model to see what the expected deviation would be for each nozzle. Fig. 5 show the results from the single nozzle configuration together with the HySafer model for each nozzle. The nozzle diameters that was tested in Fig. 5 was 0.0005m ($dz_{0.5}$), 0.0010m (dz_1) and 0.0020m (dz_2). The 0.0020m nozzle had the lowest

deviation, with an average deviation of 3.76%. Largest deviation was found with the 0.00050m nozzle, with an average relative deviation of 22.1%. The flame was unable to stabilize and blow off occurred with pressures between 3 MPa and 0.1 MPa with the 0.0005m nozzle. These are the same results obtained in [3]. The measured flame lengths in Fig 5, Fig 6 and Fig 7 includes the standard deviation of the measurement as error bars.

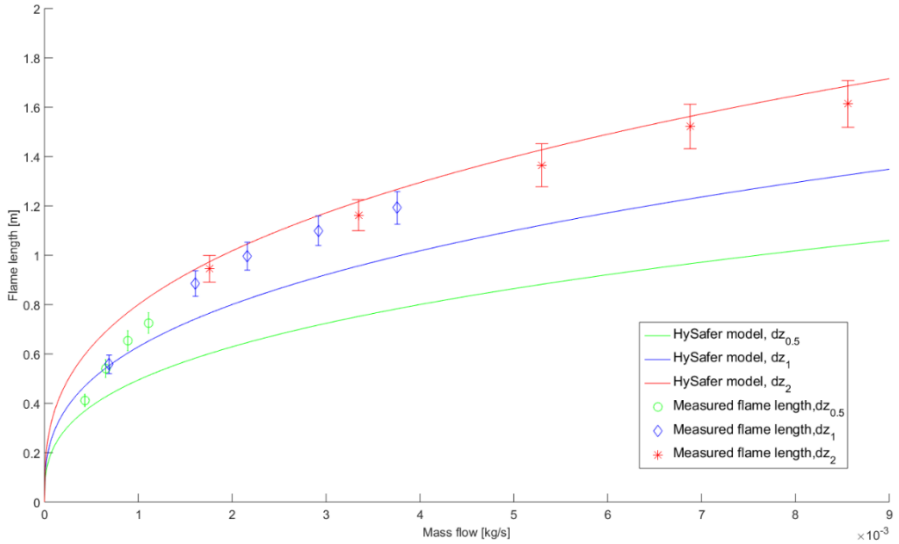

Figure 5. Single nozzle configuration results compared to HySafer model.

Fig. 6 show the comparison with a constant upstream nozzle and with a different or none downstream nozzle. Fig. 6 shows that an increase in downstream nozzle diameter increases the flame length, especially at low mass flow rates. As the mass flow increases the difference in flame length between the nozzles geometries reduces. The largest difference was found with 0.0005m nozzle upstream with 0.0040m nozzle downstream, giving a an increase in flame length of 73.5%.

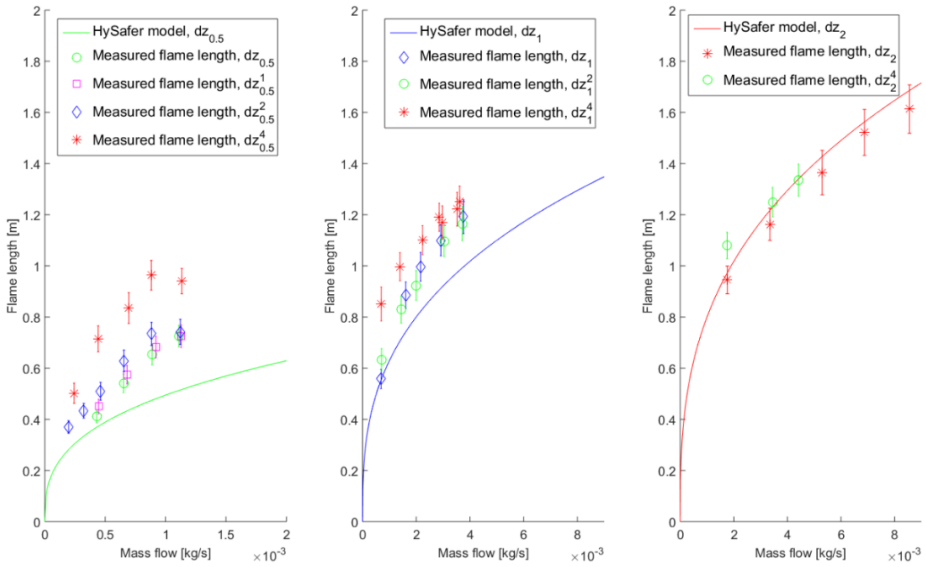

Figure 6. Constant upstream nozzle configuration with different downstream nozzle, Left: 0.0005m upstream nozzle, middle: 0.0010m upstream nozzle, right: 0.0020m upstream nozzle

By introducing a nozzle larger than 0.0010m downstream of the 0.0005m nozzle, the jet was able to stabilize and blow off did not occur. The results of the stabilized flame below 3MPa with a 0.0005m upstream nozzle and a large downstream nozzle (0.0020m and 0.0040m), is shown in the left graph in Fig. 6 as the points below a mass flow of 0.0005 kg/s.

Fig. 7 show the comparison with a constant downstream nozzle with a different or none upstream nozzle. The graphs in Fig. 7 show that the comparison with the least deviation is found in the middle graph, with and constant downstream nozzle of 0.0020m. The deviation for the two other constant downstream configurations (0.0010m, 0.0040m) are still within the error margin of 20% reported in [8].

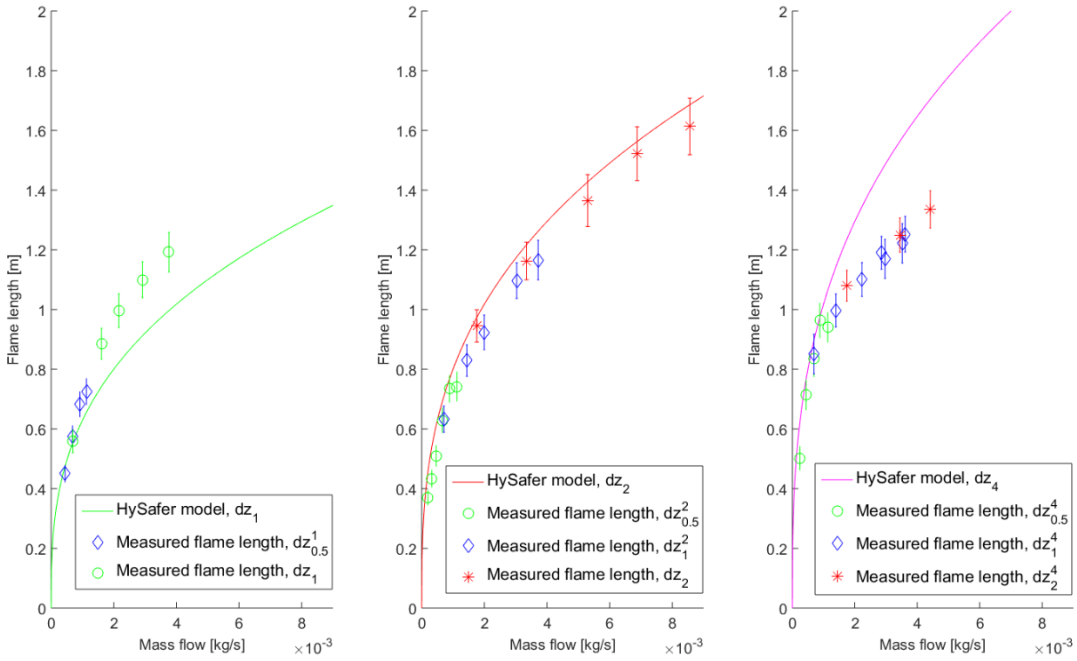

Figure 7. Constant downstream nozzle configuration with different upstream nozzle. left: 0.0010m downstream nozzle, middle: 0.0020m downstream nozzle, right: 0.0040m downstream nozzle

In the right graph of Fig. 7, the single nozzle with 0.0040m diameter was not tested. This was due to available hydrogen from one single gas cylinder would depleted too rapidly without any steady pressures and also for HSE reason since the experiments was perform indoors.

The discharge coefficient (C_0) was calculated from the choked flow equation (equation 3) and using abel-nobel equation of state to determine the compressibility factor. [9, 10]. Fig. 8 show the calculated discharge coefficient for all experiments.

$$C_0 = \frac{\dot{m}_{H_2}}{A_{dz} \cdot p_{H_2} \cdot \sqrt{\frac{\gamma_{H_2}}{R_{H_2} \cdot Z_{H_2} \cdot T_{H_2}} \cdot \left(\frac{2}{\gamma_{H_2}+1}\right)^{\frac{\gamma_{H_2}+1}{\gamma_{H_2}-1}}}} \tag{3}$$

where C_0 – discharge coefficient, [-]; $\dot{m}$ – mass flow, kg/s; A – nozzle area, m^2, p – pressure, Pa, γ - gamma (1.41), [-], Z – compressibility factor, [-], T – temperature, K.

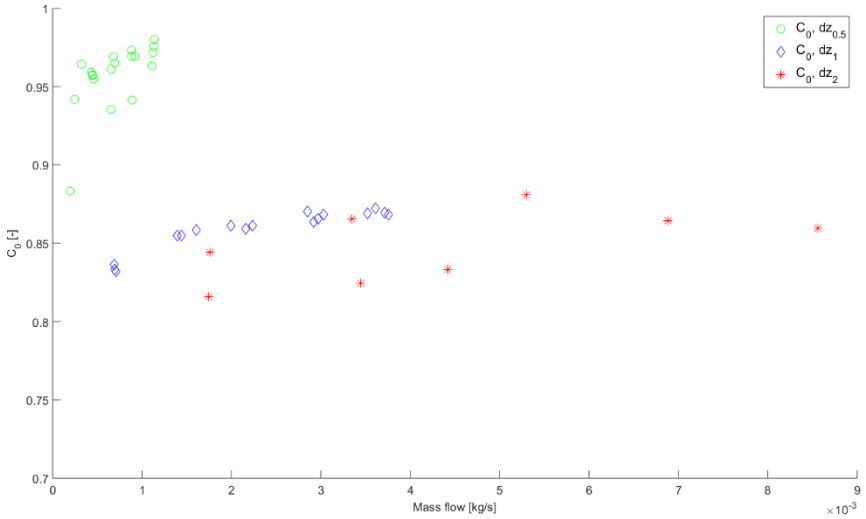

Figure 8. Discharge coefficient, circle – constant 0.0005m upstream nozzle, diamond – constant 0.0010m upstream nozzle, Asterisk – constant 0.0020m upstream nozzle

4.0 DISCUSSION

The results from Fig. 5 show a trend between the measured average flame lengths regardless of nozzle size. The trend for the single nozzle experiment indicates that the flame length is dependent of mass flow and not on the nozzle size. This is the same relationship that was found in [3, 4], but with different constants. Equation 4 is curve fitted expression of all single nozzle experiment with a coefficient of determination (R^2) value of 0.9872. The three models ([3, 4] and equation 4) is presented in Fig. 9.

$$L_f = 11.48\dot{m}^{0.406} \tag{4}$$

where L_f – flame length, m, *11.48* – constant, [-], $\dot{m}$; – mass flow, kg/s; *0.406* – constant, [-].

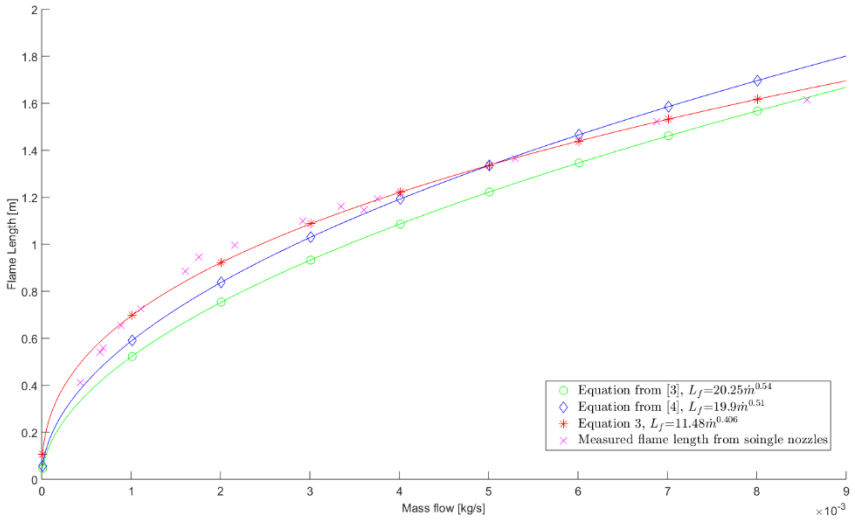

Figure 9. Comparison of the curve fitted models from [3], [4] and equation 4 with the measured flame lengths with single nozzle configuration.

Fig. 6 show that there is an increase in flame lengths when a larger nozzle is placed downstream from the critical nozzle and that the flame length increases with the increase of downstream nozzle diameter. The increase in flame length seems highest at lower mass flow rates and as the mass flow increases the effect decreases. The contribution of the larger downstream nozzle at higher mass flows must be investigated further to see if the effect continues to decrease. There is also a question of how large the diameter of the downstream nozzle can be, before having little to no effect on the flame length.

By using the equations above in Fig. 9 for a "complex" nozzle geometry can cause high deviation from the actual flame length. This can also be seen in Fig. 6 when the HySafer model is used with the upstream nozzle and not with the downstream nozzle. A relative deviation as high as 50.9% is calculated for the downstream nozzle of 0.0040m and an upstream nozzle of 0.0005m. By using equation 4 gives a lower relative deviation (32.1%), but still a high deviation.

Fig. 7 shows a trend that the downstream nozzle is determining the flame length together with mass flow. By using the downstream nozzle in the HySafer model, the flame lengths are estimated more accurately as shown in Fig. 7. The experiment with the lowest deviation was with a downstream nozzle of 0.0020m. The HySafer model under predicts for 0.0010m and over predicts for 0.0040m, but is still within the accuracy of 20%.

The nozzles with a diameter of 0.0005m has an average C_0 value of 0.96 which fits well with Fig. 8. One point is excluded in averaging of the 0.0005m experiment and that is the low value of 0.88. By examining the mass flow, large fluctuations was seen. The standard deviation for that value was calculated to 0.2, which is five times higher than the other values on average.

For the 0.0010m nozzle the average C_0 was calculated to be 0.86 and 0.84 for 0.0020m diameter nozzle. For 0.0020m diameter nozzle, the C_0 value drop with 0.02 when a large nozzle was placed downstream. This may indicate that larger nozzle has an effect on the mass flow, but more experiments needs to be performed before this can be established.

5.0 CONCLUSION

The method developed for analysing the data from each experiment has an advantage of analysing a large data set with relatively short computation time. The flame lengths found by the image-processing tool is in good agreement with manually checking the images. The drawback is that it does not relate the flame to anything physical, but rather distinguishes background noise in image and from flame. This makes the thresholding of the image crucial to the process and vital for an accurate determination of the flame length.

From the results gathered, it shows that the nozzle configuration has an effect on the flame length and stabilization of the hydrogen jet. The increase in flame length was higher at low mass flows as Fig. 6 show. The maximum percentage of increase in flame length was recorded to be 73.5%, when comparing a single nozzle configuration to a complex nozzle configuration. The effect that the downstream nozzle has on flame length may be reduce as the mass flow increases, as seen in Fig. 6, but more experiments need to be conducted for verification.

The HySafer model estimated the flame length close to the 20% error margin when the downstream nozzle was used for all experiments. Relative deviation as high as 50.9% was calculate when the upstream nozzle diameter was used, which corresponds to a large under estimation of the actual flame length. This is may be valuable input when using these models to estimate risk and safety distances from potential leak sources.

REFERENCES

1. TÜV SÜD - *Newsletter - 54 new hydrogen refuelling stations worldwide in 2015* [Online] Available at http://www.tuev-sued.de/company/press/press-archive/54-new-hydrogen-refuelling-stations-worldwide-in-2015 [Accessed on 04 of January 2017]
2. D. Baraldia, D. Melideoa, A. Kotchourkob, K. Renb, J. Yanezb, O. Jedickeb, S.G. Giannissic, I.C. Toliasc, A.G. Venetsanosc, J. Keenand, D. Makarovd, V. Molkovd, S. Slatere, F. Verbeckef, A. Duclosf, Development of a model evaluation protocol for CFD analysis of hydrogen safety issues the SUSANA project. *International Journal of Hydrogen Energy*, **xxx**, 2016, pp. I-II.
3. Mogi T., Nishida H., Horiguchi S., Flame Characteristics of high-pressure hydrogen gas jet. 1st international conference on hydrogen safety, Pisa; 2005
4. Tomohiko I., Shota H., Toshia M., Yuji W., Sadashige H., Atsumi M., Terushige O., Experimental investigation othe thermal properties of hydrogen het flame and hot current in the downstream region. *International Journal of Hydrogen* Energy, **33**, 2008, pp. 3426-3435.
5. M. Henriksen, D. Bjerketvedt, K. Vaagsaether, A.V. Gaathaug, T. Skjold, P. Middha, Accidental hydrogen release in a gas chromatograph laboratory: A case study, *International Journal of Hydrogen Energy*, **xxx**, 2016, pp. I-6.
6. R.W. Schefer W.G. Houf, T.C. Williams, B. Bourne, J. Colton, Characterization of high-pressure, underexpanded hydrogen-jet flames. *International Journal of Hydrogen* Energy, **32**, 2007, pp. 2081-2093.
7. R.W. Schefer, W.G. Houf, B. Bourne, J. Colton, Spatial and radiative properties of an open-flame hydrogen plume. *International Journal of Hydrogen* Energy, **31**, 2006, pp. 1332-1340.
8. Saffers, J. B., Molkov, V.V., Towards hydrogen safety engineering for reacting and non-reacting hydrogen releases, *Journal of Loss Prevention in the Process Industries*, **26**, 2013, pp. 344-350.
9. Daniel A.C. Joseph F.L., Chemical Process Safety Fundamentals with Application, Second Edition, 2007, Prentice Hal PTR, pp. 130-133.
10. Johnston, I.A, The Noble-Abel equation of state: Thermodynamic derivations for ballistics modelling, *Defence Science and Technology Organization* (DSTO-TN-0670)